

Imprints of the redshift evolution of double neutron star merger rate on the signal to noise ratio distribution

Shilpa Kastha^{1,2} and K. G. Arun²

¹*Institute of Mathematical Sciences, HBNI, CIT Campus, Chennai, 600113, India*

²*Chennai Mathematical Institute, Plot H1, SIPCOT IT Park, Siruseri, 603103 Tamilnadu, India*

(Dated: July 26, 2022)

Proposed third generation gravitational wave (GW) interferometers such as Einstein Telescope will have the sensitivity to observe double neutron star (DNS) mergers up to a redshift of ~ 2 with good signal to noise ratios. We argue that the measurement of *redshifted signal to noise ratio* defined by $\sigma = \rho(1+z)^{1/6}$, where ρ is the signal to noise ratio (SNR) of a detected GW event and z is its redshift can be used to study the distribution of DNS mergers. We show that if the DNS binaries are distributed uniformly within the co-moving volume, the distribution of redshifted SNR, σ , will be inversely proportional to the fourth power of σ , $p(\sigma) \propto \frac{1}{\sigma^4}$. We argue that the redshift evolution of DNS mergers will leave imprints on the distribution of σ and hence this may provide a method to probe their redshift evolution. Using various parametric models for evolution of co-moving merger rate density as a function of redshift and assuming the sensitivity of Einstein Telescope, we discuss the distinguishability of the σ distributions of these models with that of constant co-moving number density of the mergers.

I. INTRODUCTION

The first two observation runs of advanced LIGO and Virgo interferometers have led to the detections of five binary black hole mergers [1–5] and a binary neutron star merger [6]. The binary neutron star merger was also observed in various bands of the electromagnetic spectrum from gamma rays to the radio [7]. These detections have given us unique insights about the astrophysics [8–11], cosmology [12] and fundamental physics [2, 3, 11, 13]. With the planned upgrades of advanced LIGO and other similar interferometers (Virgo [14], KAGRA [15], LIGO-India [16]) joining the world-wide network of GW detectors, we are gearing up for exciting times in GW astronomy. There are ongoing research and development activities towards third generation ground-based detectors such as Einstein Telescope (ET) [17, 18] and Cosmic Explorer. Following the success of LISA Pathfinder [19], the LISA mission is now funded [20]. With these developments, GW astronomy is going to be a very active field of research in the coming decades [21].

In addition to the direct extraction of source parameters using parameter estimation algorithms, the signal to noise ratios of the observed GW events may carry a wealth of astrophysical informations. Recently Schutz [22] pointed out, on very general grounds, that the observed signal to noise ratio (SNR) of the GW events detected by GW detectors should follow a universal distribution, provided the underlying spatial density of the source population is constant within the volume accessible to the detectors. This distribution is independent of the type of the sources and hence referred to as universal. As argued by Schutz [22], the universality arises from the fact that the SNR of the GW events are inversely proportional to the luminosity distance ($\rho \propto \frac{1}{D}$) and at relatively low redshifts (say, $z \lesssim 0.3$) the luminosity distance and co-moving distance can be approximated to be the same. More precisely, following Chen and Holz [23], the probability of a source (say a compact binary merger) to be found within a shell of thickness dD , at a co-moving distance of D , goes as $f_D dD \propto D^2 dD$, if the co-moving number density of the source population is constant. Since $\rho \propto \frac{1}{D}$, the distribution of SNR corresponding to the

particular source distribution, can easily be shown to follow $p(\rho) = f_D \left| \frac{dD}{d\rho} \right| \propto \frac{1}{\rho^4}$. After normalization, we obtain

$$p(\rho) = \frac{3\rho_{th}^3}{\rho^4}, \quad (1.1)$$

where ρ_{th} is the SNR threshold used for detection. The above derivation crucially assumes that the properties of the source population (such as mass distribution) do not evolve with redshift. Chen and Holz [23] explored various implications of this universal distribution for the sources detectable by second generation detectors such as advanced LIGO/Virgo. This universal distribution is also an ingredient used in [9] to derive a bound on the rate of the binary black hole mergers from the first observation run of LIGO [2].

Motivated by [22] and [23], in this paper, we study the SNR distribution of compact binary mergers but for cosmological sources. For binary black hole mergers, their mass distribution is likely to influence the SNR distribution as much as the cosmological evolution which makes it difficult to disentangle the two effects. Hence, in order to ensure that the effect of mass distribution is minimal, here we restrict to the case of double neutron star (DNS) mergers. The planned Einstein Telescope (ET) will have enough sensitivity to detect DNS mergers with good SNR (~ 8) up to a redshift of ~ 2 [17, 18]. DNS mergers are exciting as they are confirmed to be progenitors of short Gamma Ray Bursts (SGRBs) [11, 24].

For DNS mergers detectable by ET, we show that a new quantity, called *redshift scaled SNR* (or simply redshifted SNR) denoted by $\sigma = \rho(1+z)^{1/6}$, where z is the redshift of the source, can be shown to follow a $\frac{1}{\sigma^4}$ distribution provided their number density is constant within the co-moving volume accessible to the detector. We then discuss how potential deviations from this *reference* $\frac{1}{\sigma^4}$ distribution can be used to track the redshift evolution of the rate density of DNS mergers. Considering certain parametrized models for the redshift evolution of DNS merger rate density, we study how distinguishable are the resulting distributions of σ from the reference $\frac{1}{\sigma^4}$ distribution. In practice, one would be interested in the inverse problem of determining the rate density of DNS mergers as a function of the redshift. We briefly discuss how this can be done, leaving

a detailed analysis to a future work.

The paper is organized in the following way. In Sec. II we consider the cosmological effects on the optimal SNR of compact binary sources and construct a new quantity, redshifted SNR. We further discuss about the distribution of this redshifted SNR for DNS mergers which are distributed uniformly within the co-moving volume. In Sec. III we explore how the different DNS merger rate densities affect the redshifted SNR distributions and whether the distributions corresponding to all the merger rate densities are distinguishable from the reference one obtained from uniform source population. We conclude our study by discussing about several factors that may affect our analysis.

II. COSMOLOGICAL EFFECTS ON THE SIGNAL TO NOISE RATIO DISTRIBUTION

The data analysis technique of matched filtering [25, 26] is usually employed to detect compact binary mergers using GW observations. Matched filtering involves cross-correlating various copies of the expected gravitational waveforms (tem-

plates), which correspond to different signal parameters (such as masses and spins), with the data, which potentially contains the signal (in addition to the noise). The template which maximizes the correlation is referred to as optimal template and the corresponding signal to noise ratio is called optimal SNR which is defined as

$$\rho = \sqrt{4 \int_0^\infty \frac{|\tilde{h}(f)|^2}{S_h(f)} df}, \quad (2.1)$$

where $S_h(f)$ is the detector's power spectral density (PSD) and $\tilde{h}(f)$ is the frequency domain gravitational waveform (See, for instance, Sec. (5.1) of [21] for details).

We employ restricted post-Newtonian (PN) waveform (RWF), $\tilde{h}(f) = \mathcal{A} f^{-7/6} e^{i\psi(f)}$, where \mathcal{A} is the amplitude and $\psi(f)$ is the frequency domain GW phase. In RWF, the PN corrections to the amplitude of the gravitational waveform are ignored but the phase is accounted for to the maximum accuracy. Using the RWF, the optimal SNR for GW events of compact binary systems can be written as [27]

$$\rho(m_1, m_2, D_L, \theta, \phi, \psi, \iota) = \sqrt{4 \frac{\mathcal{A}^2}{D_L^2} [F_+^2(\theta, \phi, \psi)(1 + \cos^2 \iota)^2 + 4F_\times^2(\theta, \phi, \psi) \cos^2 \iota]} I(M), \quad (2.2)$$

where $F_{+, \times}(\theta, \phi, \psi)$ are the antenna pattern functions for the 'plus' and 'cross' polarizations, $\mathcal{A} = \sqrt{5/96} \pi^{-2/3} \mathcal{M}^{5/6}$, \mathcal{M} is the chirp mass, which is related to the total mass by $\mathcal{M} = M\eta^{3/5}$, where $\eta = \frac{m_1 m_2}{M^2}$ is the symmetric mass ratio of the system and m_1, m_2 are the component masses. $I(M)$ is the frequency integral defined as

$$I(M) = \int_0^\infty \frac{f^{-7/3}}{S_h(f)} df \simeq \int_{f_{low}}^{f_{LSO}} \frac{f^{-7/3}}{S_h(f)} df. \quad (2.3)$$

In the last step, we have replaced the lower and upper limit of the integral by the seismic cut off, f_{low} , of the detector and the frequency at the last stable orbit of the black holes with masses m_1 and m_2 , respectively. The GW frequency at the last stable orbit (LSO) upto which PN approximation is valid, as a function of the total mass M is, $f_{LSO} = \frac{1}{6^{3/2} \pi M}$. This is the expression for the LSO of a Schwarzschild BH with total mass M . We next address the effect of cosmological expansion on the SNR and its distribution.

A. Modifications due to cosmological effects

Assuming a flat FRW cosmological model for the universe, we explore the modification to the SNR for compact binary systems at cosmological distances. Cosmological expansion of the universe affects the gravitational waveforms in two ways. According to general relativity, GW amplitude is inversely proportional to the co-moving distance D , which is

no longer same as the luminosity distance D_L but is related by $D_L = D(1+z)$ (for flat FRW cosmology), where z is the redshift of the source. Secondly, the gravitational wave frequency is redshifted. Both of these effects get translated into a redefinition of the chirp mass. The observed chirp mass (\mathcal{M}), is related to the corresponding chirp mass in the source frame (\mathcal{M}_{source}), by $\mathcal{M} = \mathcal{M}_{source}(1+z)$. This happens due to the fact that the only time scale of the problem $\frac{GM}{c^3}$, is redshifted, which is completely degenerate with mass and hence leading to the notion of redshifted mass (see Sec. 4.1.4 of [28]). Since redshift for a given cosmological model is written as a non-linear function of the distance, it is obvious that the simple scaling relations which lead to the universal SNR distribution (see Eq. (1.1)) do not apply any more. Though the distribution of SNR is not universal, one can still ask if there exists a quantity which goes as $1/D$ so that there is a universal distribution in a new quantity.

After accounting for the cosmological effects in the gravitational waveform, mentioned above, the expression for SNR schematically reads

$$\rho = \frac{\mathcal{M}_{source}^{5/6}}{D(1+z)^{1/6}} g(\theta, \phi, \psi, \iota) \sqrt{I(M)}, \quad (2.4)$$

where all the angular dependencies in the waveform are captured into the definition of $g(\theta, \phi, \psi, \iota)$ and other variables have their usual meanings. One may note from Eq. (2.4) that, we can define a new variable $\sigma = \rho(1+z)^{1/6}$ which depends inversely on the co-moving distance, like SNR did earlier with

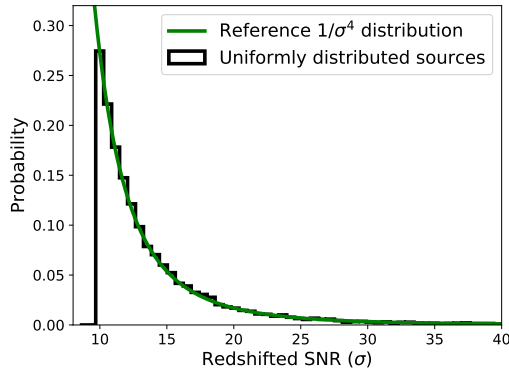


FIG. 1: The figure shows the excellent agreement between the redshifted SNR distribution for DNS mergers from a simulated population which is uniformly distributed in the co-moving volume upto the redshift reach of Einstein telescope ($z_{max} \approx 2.1$) for an SNR threshold of 8 with that of the analytical prediction in Eq. (2.6).

luminosity distance. More explicitly,

$$\sigma = \frac{M_{\text{source}}^{5/6}}{D} g(\theta, \phi, \psi, \iota) \sqrt{I(M)}. \quad (2.5)$$

Though we have absorbed all the redshift dependences into the definition of redshifted SNR, σ , the integral $I(M)$, which needs to be numerically evaluated, still has a redshift dependence. However for sufficiently small masses which are not at very high redshifts, it can be shown that the redshifted mass in the above integral can very well be approximated by the mass in the source frame, M_{source} . If we restrict ourselves to the low mass regime, say DNS systems with total mass of $\leq 3M_{\odot}$, the relative difference between $\sqrt{I(M_{\text{source}})}$ and $\sqrt{I(M)}$ is only of the order of 0.55% for sources in the ET sensitivity band up to a redshift of ~ 2.37 . Hence, for a uniform population of DNS mergers within the co-moving volume, the normalized redshifted SNR distribution (analogous to the SNR distribution of see Eq. (1.1) reads

$$p(\sigma) = \frac{3\sigma_{\text{th}}^3}{\sigma^4}, \quad (2.6)$$

where $\sigma_{\text{th}} = \rho_{\text{th}}(1 + z_{\text{max}})^{1/6}$ is the threshold on redshifted SNR and z_{max} is the redshift reach with the ρ_{th} as SNR threshold. This threshold on σ means that not all sources which pass the SNR threshold ρ_{th} would pass the threshold for redshifted SNR, but the converse is always true.

There is one important point to note here. As mentioned earlier, due to the degeneracy between the total mass and GW frequency, GW observations cannot infer redshift directly. One scenario where independent redshift information will be available is the case if the DNS merger is accompanied by an electromagnetic emission which is observed and used to infer the redshift of the source. However this will be a subset of the total DNS mergers observed. Another proposal to obtain redshift from GW observations alone is to invoke the higher order corrections to the phasing which involves terms that depend on the equation of state of the NS which breaks the degeneracy between the mass and the redshift making the redshift estimation possible [29]. In this work, we simply use the fact that ET will

be able to measure the luminosity distance to the DNS mergers rather accurately and using a cosmological model, this can be converted to redshift. Since we are not interested in testing the cosmological parameters, this procedure would suffice. Hence, in order to get a distribution of redshifted SNR, we need, in addition to the SNR of the corresponding the detections, an accurate parameter estimation of the distance, which in turn leads to an estimate of the redshift.

According to flat FRW cosmology, the luminosity distance of a source in $c = G = 1$ unit at a redshift of z (Ref. [30]) is

$$D_L(z) = \frac{(1+z)}{H_0} \int_0^z \frac{dz'}{E(z')}, \quad (2.7)$$

where

$$E(z) = \sqrt{\Omega_m(1+z)^3 + \Omega_\Lambda}, \quad (2.8)$$

and the total density parameter (Ω) consists of matter (dark and baryonic) density (Ω_m) and cosmological constant (Ω_Λ). Based on various cosmological observations, we consider $\Omega_\Lambda = 0.7$ and $\Omega_m = 0.3$ and the Hubble constant $H_0 = 72\text{km/Mpc/sec}$ for our analysis. We numerically invert the above expression to obtain the redshift value for a given luminosity distance. We assume the errors in estimating the luminosity distance and redshift are negligible (see Sec. IV for a detailed discussion of the effects of errors in luminosity distance, on the redshifted SNR distribution).

For the signal to noise ratio computations, we have used Einstein Telescope sensitivity curve of Ref. [18] which reads

$$S_h^{1/2}(f) = s_0^{1/2} [a_1 x^{b_1} + a_2 x^{b_2} + a_3 x^{b_3} + a_4 x^{b_4}] \text{ for } f \geq f_s, \\ = \infty; f < f_s, \quad (2.9)$$

where $x = f/f_0$, $f_0 = 100\text{Hz}$, $f_s = 1\text{Hz}$, $f_{\text{LSO}} = (6^{3/2}\pi M)^{-1}$ and $s_0 = 10^{-50}\text{Hz}^{-1}$, $a_1 = 2.39 \times 10^{-27}$, $a_2 = 0.349$, $a_3 = 1.76$, $a_4 = 0.409$, $b_1 = -15.64$, $b_2 = -2.145$, $b_3 = -0.12$ and $b_4 = 1.10$.

We next simulate the detections of DNS mergers with constant co-moving number density by ET. In order to generate such a source population, the sources are assumed to be uniformly located and oriented on the two-sphere. This is achieved

by making sure that the azimuth angles ϕ, ψ are drawn from a uniform distribution $[0, 2\pi]$ and the polar angles θ, ι are chosen such that their cosines are uniformly distributed between $[-1, 1]$. These choices ensure that at any radius, the source population is uniformly located and oriented on the surface of the sphere. Further, we need to distribute the sources uniformly *within* the detection volume specified by the maximum radius $D_{\max}(\rho_{\text{th}}, M)$ (or $z_{\max}(\rho_{\text{th}}, M)$), which depends on the SNR threshold. In order to get the above mentioned uniformity of the source population, we choose the co-moving distance D in such a way that D^3 is uniform in the closed interval $[0, (D_{\max})^3]$.

For each realization of this population, we compute the redshifted SNR (assuming no error on luminosity distance and cosmological parameters). The sources which are relevant for our purpose are those which cross the threshold on the redshifted SNR. The threshold on the redshifted SNR for a given population with fixed total mass M is defined by

$$\sigma_{\text{th}}(M, \rho_{\text{th}}) = \rho_{\text{th}} \left[1 + z_{\max}(\rho_{\text{th}}, M) \right]^{1/6}, \quad (2.10)$$

where $z_{\max}(\rho_{\text{th}}, M)$ is the redshift reach for the system (in our case DNS systems with $M = 2.8M_{\odot}$) for a fixed SNR threshold (8 in our case). This means that not all sources which cross the SNR threshold from the Monte Carlo will survive redshifted SNR threshold (σ_{th}) but all, those which survive our σ_{th} will have $\rho \geq \rho_{\text{th}}$. We find that of all the sources which cross the detection threshold, approximately 80% of them would also cross the σ_{th} .

Fig. 1 explicitly shows the distribution of redshifted SNR for a population of DNS systems whose spatial distribution is uniform within the co-moving volume of the Einstein Telescope detector which has a $z_{\max} \simeq 2.1$ (for an SNR threshold of 8). The distribution derived from the Monte Carlo simulations mimicking the detection of DNS mergers which are distributed uniformly in the co-moving volume is superimposed on the theoretically predicted $p(\sigma)$ distribution given in Eq. (2.6) to show excellent agreement. Fig. 1 is generated with about 8850 redshifted SNR samples among 10961 detected events.

III. EVOLUTION OF CO-MOVING MERGER RATE DENSITY OF DNS SYSTEMS AND THEIR IMPRINTS ON THE REDSHIFTED SNR DISTRIBUTION

In the previous section we have obtained the distribution of redshifted SNR for DNS merger population which has constant co-moving number density. We now derive the distribution of redshifted SNR for various models in which the DNS merger rate density evolves as a function of the redshift. We then discuss the corresponding redshifted SNR distributions and how one can use these to infer the properties of the redshift evolution of the source population.

Let $R(z) = R_0 f(z)$ be the schematic form of redshift evolution of merger rate density, where R_0 is some constant of normalization (physically, R at some reference redshift z_0) to be fixed. We use the empirical models, motivated by the short gamma ray burst literature [31, 32], for the redshift evolution of DNS mergers, which reads,

$$R(z) = R_0 \left(\frac{1+z}{1+z_0} \right)^{\alpha}, \quad (3.1)$$

where

$$\alpha = \alpha_1 \quad \text{for } z \leq z_0, \quad (3.2)$$

$$\alpha = \alpha_2 \quad \text{for } z > z_0, \quad (3.3)$$

where R_0 is the rate density at $z = z_0$. Assuming the sources are isotropically distributed, the total number of sources in a co-moving volume of radius D is,

$$N(D) \propto \int_0^D \frac{R(z(D'))}{1+z(D')} D'^2 dD', \quad (3.4)$$

where z can be numerically inverted to obtain the corresponding co-moving distance. The $(1+z)$ factor in the denominator takes care of the effect of cosmological time dilation of the interval between the detected sources. When multiplied by the time of observation, N becomes the number of mergers in the co-moving volume up to a maximum distance in the given observation time.

In this paper we have used three sets of different parametrizations as the models for binary merger rate density evolution (see left panel of Fig. 2). We fix $R_0 = 2\text{Mpc}^{-3}\text{Gyr}^{-1}$ to be fixed for all the models.

- Model 0: $\alpha_1 = \alpha_2 = 1, z_0 = 1$,
- Model 1: $\alpha_1 = 2, \alpha_2 = -5, z_0 = 0.5$,
- Model 2: $\alpha_1 = 2, \alpha_2 = -5, z_0 = 1$,
- Model 3: $\alpha_1 = 4, \alpha_2 = 1, z_0 = 1$.

Model 0 represents the evolution of rate density corresponding to the source population which is uniform in the co-moving volume. The choices of α_1 and α_2 for the other three, model the different scenarios where rate density increases or decreases with redshift before or after z_0 . The z_0 itself may be different for different models. Left panel of Fig. 2 shows three representative merger rate density functions discussed above.

Considering these models to be the underlying source distribution within the co-moving volume and assuming isotropy, we obtain the redshifted SNR distribution of DNS mergers for ET (right panel Fig. 2). To generate the source population for obtaining the redshifted SNR distributions corresponding to different $R(z)$ (left panel of Fig 2), we follow the similar procedure as described earlier to obtain Fig 1. The only difference here is the way of assigning the co-moving distance for the elements of the population. Here, as opposed to the earlier case, we choose $N(D)$ to be uniformly distributed between $N(1)$ and $N(D_{\max})$ and for each realization, we numerically solve Eq (3.4) to obtain corresponding D value from $N(D)$ and we also make sure that we choose the particular solution which does not exceeds D_{\max} . This eventually gives rise to a rate density as shown in Eq. (3.1) for a large number of realizations. With the source population obtained from simulation described above, we calculate the redshifted SNR for each source. Discarding all the redshifted SNR values which do not cross the threshold in Eq. (2.10), we obtain the distribution of

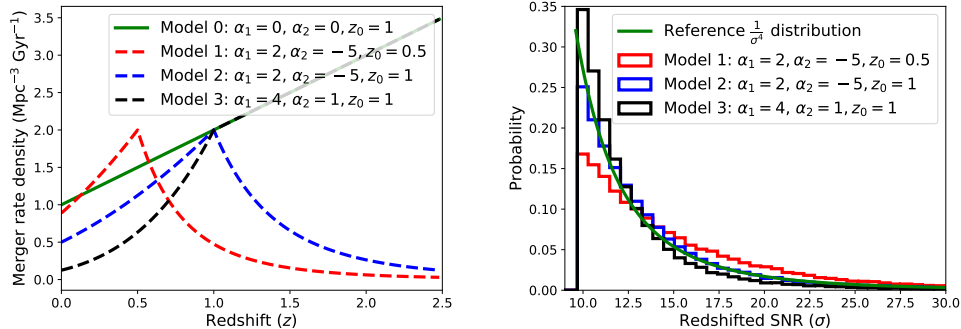


FIG. 2: Figure on the left panel shows the evolution of co-moving merger rate density with redshift (see Eq. 3.1) for three different models. Figure on the right panel shows the corresponding redshifted SNR distributions. The rate density for Model 0, corresponding to the uniform source distribution, is also shown in the left panel which produces the reference redshifted SNR distribution ($1/\sigma^4$) (Eq. 2.6) on the right panel. For all of these models $R_0 = 2\text{Mpc}^{-3}\text{Gyr}^{-1}$.

redshifted SNR shown in the right panel of Fig 2. It contains the distributions of redshifted SNR for various models together with the reference distribution, $p(\sigma) = \frac{3\sigma^3}{\sigma^4}$. Next we discuss how many detections are required for these models to be statistically distinguishable from the reference distribution which correspond to constant co-moving number density.

A. Statistical tests

We use Anderson-Darling (AD) [33] test to quantify the distinguishability of the three merger rate density models from the reference model of constant co-moving number density. The AD test measures whether a sample data (in our case a given distribution of σ for a parametric model) came from a specific distribution (reference $\frac{1}{\sigma^4}$ distribution). The test returns a probability value (p value) for the “null” hypothesis that *sample belongs to the reference distribution*. If the null hypothesis is true, the p value distribution is uniform between 0 and 1. If the sample does not belong to the reference distribution, the p value distribution will sharply peak around 0. A p value distribution weighted more towards 0, implies a stronger evidence of rejecting the null hypothesis or ability to distinguish the two distributions.

To perform the tests, we generate a set of redshifted SNR samples with 20, 50, 100, 200, 500, 1000 detections. Each detected sample, with the fixed number of detections, are generated 100 times from the source distribution in the co-moving volume that follows the various rate models mentioned earlier. For these 100 copies of the particular set, we carry out the AD test and calculate the median p values. We perform the same exercise on the six set of detection samples and plotted as a function of detection number (see Fig. 3). In order to pictorially illustrate that the p value distributions are weighted more towards 0, we fix the number of detection to be 100 for the three models. We perform the AD test on 100 randomly generated samples for each model to obtain the histograms shown in the left panel of Fig 3. The distributions of p values for Model 1 and Model 3 are weighted more towards 0, where as for Model 2 it is more or less uniform, indicating the rejection

of null hypothesis for Model 1 and 3 only. The three different Models demonstrate different behaviours. For Model 1 and 3 it is very clear that once we increase the number of detections the median p value sharply falls to zero (see right panel of Fig 3). We found similar results with Kolmogorov-Smirnov test as well, though we do not show them here.

From the right panel of Fig. 3, it is evident that Model 1 and Model 3 can be distinguished from the reference distribution with high confidence with a few tens of detections, whereas Model 2 is very difficult to distinguish from the reference distribution using this method. This is also clear from the left panel of the same figure which shows the p value distribution of Model 2 to be uniform which shows the consistency with the null hypothesis and hence difficult to distinguish.

These results show only how distinguishable different distributions are from the reference one. When we have a bunch of observations, the way to proceed would be pose this as a parameter estimation problem where $\{\alpha_1, \alpha_2, z_0\}$ are variables to be estimated. We postpone a detailed investigation of the parameter estimation problem for a future work.

IV. CAVEATS

As mentioned earlier, this is intended to be a proof-of-principle demonstration of a method to track the redshift evolution of DNS mergers and hence we have worked with many strong assumptions. We have not included measurement errors on any quantity while studying the simulated populations used to demonstrate the idea. Moreover, here we have used the point estimates of σ to demonstrate the method. This will have to be extended to include the posterior distributions of σ for individual events, say, within the Bayesian framework to be directly applicable to the observations. In addition, there will be errors associated with masses and distance as well as calibration errors which may induce an error on the measured values of σ for individual events, all of which have been ignored here. We discuss below, somewhat quantitatively, the effect some of these errors on our scheme.

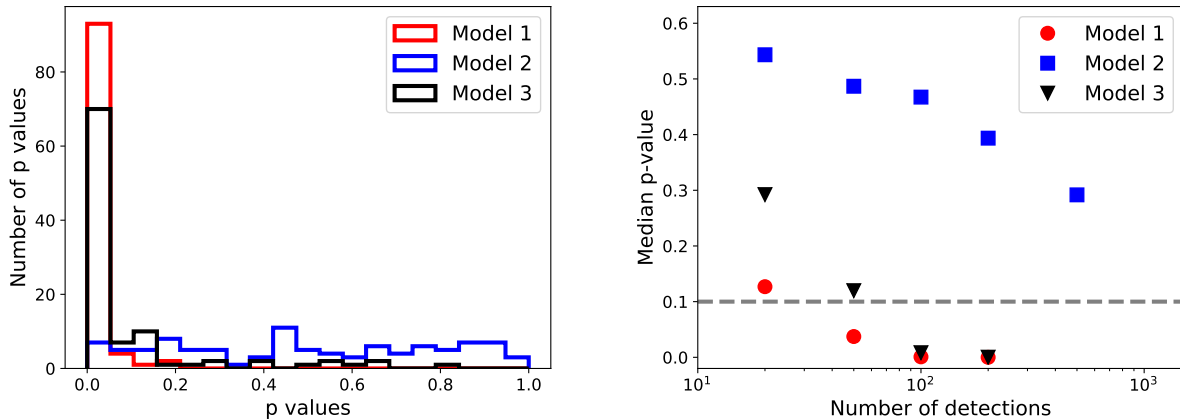


FIG. 3: Left Panel: Distribution of p values for the three models from Anderson Darling test on 100 random samples, each sample contains 100 detection on an average. Right panel: Median p-value from Anderson-Darling test performed on the data obtained from the three parametric models as function of number of detections. For Model 1, $\alpha_1 = 2, \alpha_2 = -5, z_0 = 0.5$, for Model 2, $\alpha_1 = 2, \alpha_2 = -5, z_0 = 1$ and for Model 3 $\alpha_1 = 4, \alpha_2 = 1, z_0 = 1$. For all of these models $R_0 = 2\text{Mpc}^{-3} \text{Gyr}^{-1}$.

A. Effects of uncertainty in the luminosity distance estimation

The distance measurements of ET will have error bars which we have neglected at present. Here we obtain a back of the envelop estimate for the typical error on redshifted SNR values for the uncertainty in the distance estimation. According to error propagation equation, the fractional error on redshifted SNR due to error in redshift, assuming no error on SNR, is

$$\frac{\delta\sigma}{\sigma} = \frac{\delta z}{6(1+z)}, \quad (4.1)$$

where

$$\delta z = \left(\frac{\partial D_L}{\partial z} \right)^{-1} \delta D_L \quad (4.2)$$

$$= \left[\frac{D_L}{1+z} + \frac{1+z}{H_0 \sqrt{\Omega_m(1+z)^3 + \Omega_\Lambda}} \right]^{-1} \delta D_L. \quad (4.3)$$

The above equations are in $c = 1 = G$ units (see Eq. (2.7)). If a source gets detected at a luminosity distance of 500 Mpc with 10% error bar on the distance estimation, the fractional error on σ is of the order of about 0.001, which is very small. Even if the error on D_L is as bad as 50%, the error on σ is ~ 0.007 , which is not too large either. But the errors increase by order one for the sources at the farthest, which will induce a deviation on the redshifted SNR distribution.

We have assumed flat FRW cosmological model for all of our calculations. But the variations of different cosmological parameters affects the redshifted SNR distribution. A 10% error on $H_0 (= 72 \text{ km/Mpc/sec})$ and $\Omega_\Lambda (= 0.7)$ along with 50% error on luminosity distance ($= 500 \text{ Mpc}$) give rise to a fractional error of about 0.8% on redshifted SNR. All of these assume there is no error bar on the signal to noise ratio, say from the calibration.

B. Effects of neglecting redshifted mass

As we mentioned earlier, our approximation of neglecting the redshifted mass effect, while calculating the SNR integral, Eq. (2.3), will induce a maximum error of about 0.38% on the estimation of redshifted SNR of DNS merger of total mass $2.8 M_\odot$ at the threshold value (8 here) and this estimated error eventually decreases as we move to higher redshifted SNR values or the low redshift sources, which eventually gives rise to the proposed $p(\sigma) = \frac{3\sigma^3}{\sigma^4}$ distribution. Where as, for an SNR threshold of 5, the redshift reach of the detector ≈ 4.8 . Due to this high redshift reach, corresponding error on redshifted SNR increases to 1.9%.

Further more, in our analysis so far, we have considered fixed mass DNS systems with total mass of $2.8 M_\odot$. But in reality, the total mass may vary, say, from 2 to $4 M_\odot$. A higher total mass, since the redshift reach is more, the error in σ values is also large near the threshold. We find that for a total mass of $4 M_\odot$ the relative error on the SNR is 2.4%.

V. CONCLUSIONS

We have demonstrated an interesting possibility of using the redshifted signal to noise ratios of double neutron star mergers detectable by third generation telescopes, such as ET, to infer how the source population evolves as a function of redshift. Though the proposed method may be less effective compared to the straightforward method of simply binning the events as a function of redshift [34] and estimate the parameters of cosmological evolution, this may be an interesting alternative with complementary systematics. There are ongoing efforts to develop methods, within the hierarchical Bayesian inference, to fit for the parameters describing the redshift evolution of compact binaries [35] from GW observations. We have only done of a proof-of-principle demonstration of this method which may have to be put on a more rigorous footing in order

to be applicable to real observations.

Acknowledgments

K. G. A. is partially supported by a grant from Infosys Foundation. K. G. A. acknowledges the support by the Indo-US Science and Technology Forum through the Indo-US Centre

for the Exploration of Extreme Gravity (Grant No. IUSSTF/JC-029/2016). We would like to thank Nathan Johnson-McDaniel, B. S. Sathyaprakash, P. Ajith, Chris Van Den Broeck, Archisman Ghosh, Ghanashyam Date, Alok Laddha and N V Krishendu for very valuable discussions. We thank Maya Fishbach for useful comments on the manuscript. This document has LIGO preprint number P1800002.

-
- [1] B. P. Abbott et al., Phys. Rev. Lett. **116**, 061102 (2016).
 [2] B. P. Abbott et al., Phys. Rev. Lett. **116**, 241103 (2016).
 [3] B. P. Abbott et al., Phys. Rev. Lett. **118**, 221101 (2017), 1706.01812.
 [4] B. P. Abbott et al., Phys. Rev. Lett. **119**, 141101 (2017), 1709.09660.
 [5] B. P. Abbott et al., Astrophys. J. **851**, L35 (2017), 1711.05578.
 [6] B. P. Abbott et al., Phys. Rev. Lett. **119**, 161101 (2017), 1710.05832.
 [7] B. P. Abbott et al., Astrophys. J. **848**, L12 (2017), 1710.05833.
 [8] B. P. Abbott et al., Astrophys. J. **818**, L22 (2016), 1602.03846.
 [9] B. P. Abbott et al., Astrophys. J. **833**, L1 (2016), 1602.03842.
 [10] B. P. Abbott et al., Phys. Rev. Lett. **116**, 241102 (2016), 1602.03840.
 [11] B. P. Abbott et al., Astrophys. J. **848**, L13 (2017), 1710.05834.
 [12] B. P. Abbott et al., Nature **551**, 85 (2017), 1710.05835.
 [13] B. P. Abbott et al., Phys. Rev. Lett. **116**, 221101 (2016), 1602.03841.
 [14] <http://www.virgo.infn.it>.
 [15] T. Uchiyama et al., Classical and Quantum Gravity **21**, S1161 (2004).
 [16] B. Iyer et al., LIGO-India Technical Report No. LIGO-M1100296 (2011), URL <https://dcc.ligo.org/LIGOM1100296/public/main>.
 [17] B. Sathyaprakash et al., Class. Quant. Grav. **29**, 124013 (2012), [Erratum: Class. Quant. Grav.30,079501(2013)], 1206.0331.
 [18] <http://www.et-gw.eu/>.
 [19] M. Armano et al., Phys. Rev. Lett. **116**, 231101 (2016).
 [20] S. Babak, J. Gair, A. Sesana, E. Barausse, C. F. Sopuerta, C. P. L. Berry, E. Berti, P. Amaro-Seoane, A. Petiteau, and A. Klein, Phys. Rev. **D95**, 103012 (2017), 1703.09722.
 [21] B. Sathyaprakash and B. Schutz, Living Rev. Rel. **12**, 2 (2009), arXiv:0903.0338.
 [22] B. F. Schutz, Classical and Quantum Gravity **28**, 125023 (2011), 1102.5421.
 [23] H.-Y. Chen and D. E. Holz, ArXiv e-prints (2014), 1409.0522.
 [24] R. Narayan, B. Paczynski, and T. Piran, Astrophys. J. **395**, L83 (1992), astro-ph/9204001.
 [25] C. Hellström, *Statistical Theory of Signal Detection*, vol. 9 of *International Series of Monographs in Electronics and Instrumentation* (Pergamon Press, Oxford, U.K., New York, U.S.A., 1968), 2nd ed.
 [26] L. A. Wainstein and V. D. Zubakov, *Extraction of Signals from Noise* (Prentice-Hall, Englewood Cliffs, 1962).
 [27] C. Cutler and E. Flanagan, Phys. Rev. D **49**, 2658 (1994).
 [28] M. Maggiore, *Gravitational Waves. Vol. 1: Theory and Experiments* (Oxford University Press, 2007).
 [29] C. Messenger and J. Read, Phys. Rev. Lett. **108**, 091101 (2012), 1107.5725.
 [30] D. W. Hogg (1999), astro-ph/9905116.
 [31] T. Totani, The Astrophysical Journal Letters **486**, L71 (1997).
 [32] M. Schmidt, Astrophys. J. **700**, 633 (2009), 0905.2968.
 [33] T. W. Anderson and D. A. Darling, Ann. Math. Statist. (1952).
 [34] W. Farr and S. Vitale (2018), in Preparation.
 [35] M. Fishbach and D. Holz (2018), in Preparation.